

# Performance Evaluation of a Ranque-Hilsch Vortex Tube with Optimum Geometrical Dimensions

Mohammadi, Samira; Farhadi, Fatolah\*<sup>+</sup>

Department of Chemical and Petrochemical Engineering, Sharif University of Technology, Tehran, I.R. IRAN

**ABSTRACT:** A brass Vortex Tube (VT) with interchangeable parts is used to determine the optimum cold end orifice diameter, main tube length and diameter. Experiments were carried out to study the effects of operating pressure as well. It is shown that there is an optimum value for cold end orifice diameter, which is equal to 4mm and there is an optimum value for cold and hot exit temperature difference at  $CF=0.4$ . A 2-D Computational Fluid Dynamics (CFD) model is validated against the present experimental data. CFD code is applied to investigate the role of vortex tube diameter and length on the temperature separation. The code is also used to investigate and analyze the highly rotating flow field structure and its characteristic with respect to various cold fractions. Finally the results are extrapolated for investigating the effect of inlet pressures up to 1053kPa, VT on separation performances.

**KEY WORDS:** Vortex tube; Geometrical optimization; Ranque-Hilsch.

## INTRODUCTION

A Vortex Tube (VT) is a cylindrical pipe where a compressed fluid, enters tangentially through nozzles and passes the main tube. This device (Fig.1) separates the entering fluid in two hot and cold streams. Most vortex tubes have a conical valve at one end of the tube (usually at the hot end) which adjust the cold to inlet flow ratio called the Cold Fraction (CF).

Because of simplicity, compactness and their maintenance free nature, VTs are gaining more and more attention in special applications.

Since first experiments of VT by Ranque, several theories have been advanced to explain the vortex tube's thermal behavior. Kurosaka [1], Ahlborn & Groves [2], Hilsch [3], Ahlborn & Gorden [4], Gao *et al.* [5] and Deissler & Perlmutter [6], tried to describe the thermal separation mechanism of the vortex tube.

Frohlingdorf & Unger [7], proposed a CFD model for studying compressible and turbulent effects. A 2-D flow model of mass, momentum and energy conservation equations were also solved numerically by Amitani *et al.* [8]. Aljuwayhel *et al.* [9] used a CFD model for the vortex tube to describe the basic processes leading to the flow separation. By using the standard  $k-\epsilon$  model and an algebraic Reynolds Stress Model (RSM) Eiamsa-ard & Promvong [10] reported a simulation of thermal separation in a Ranque-Hilsch Vortex Tube (RHVT).

Then, Dincer *et al.* [11] directed modeling in a vortex tube by artificial neural networks. The CFD analysis of the number of nozzles, cold end orifice diameter and length to diameter ratio effect on VT performance was studied by Behera *et al.* [12]. Xue *et al.* [13] presented a review of a VT energy separation phenomenon explanation

---

\* To whom correspondence should be addressed.

+ E-mail: farhadi@sharif.edu

1021-9986/16/1/95

13/\$/3.30

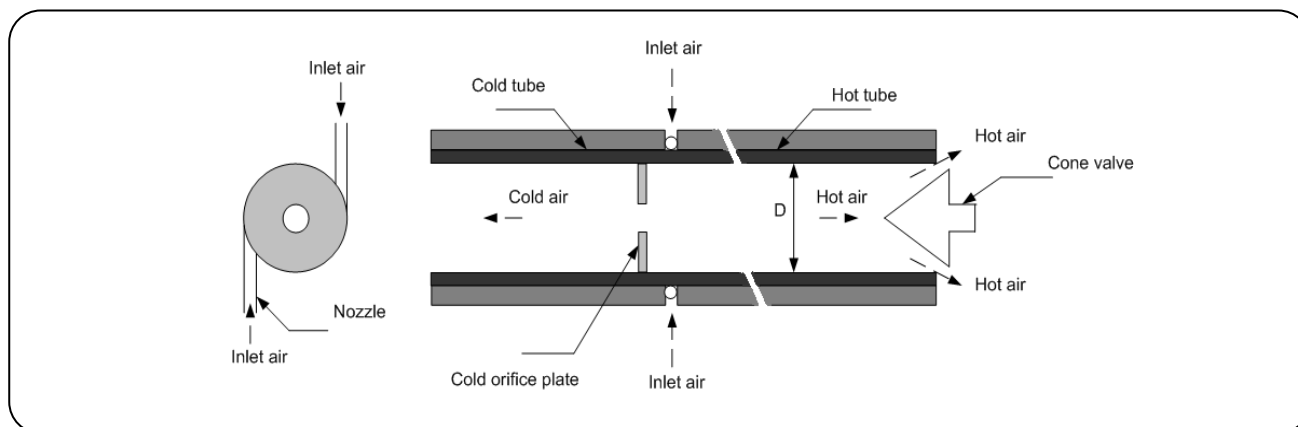


Fig. 1: Schematic diagram of a VT.

and discussed the effect of pressure, viscosity, turbulence, temperature, secondary circulation and acoustic streaming on the performance. Dutta *et al.* [14] applied different turbulence models (standard  $k-\epsilon$ , RNG  $k-\epsilon$ , standard  $k-\omega$  and SST  $k-\omega$  turbulence models) for a CFD model and obtained the performance curves. The effect of RNG  $k-\epsilon$  and a RSM turbulence models in an axis-symmetric 2-D model is also studied by Secchiaroli *et al.* [15].

Aydın & Baki [16] investigated the VT length, inlet nozzle diameter and the conical angle of the control valve effect on VT performance under different inlet pressure in a series of experiments. Nimbalkar & Muller [17] focused their experiment on the effect of different inlet pressures, cold fractions and cold end orifice diameters on VT energy separation. The effects of angle and diameter of hot end conical valve were determined experimentally by Dincer *et al.* [18].

Kirmaci [19] reported the effects of the nozzle number and the inlet pressure on the VT performance when air and oxygen are used and the exergy efficiency was reported. Aydın *et al.* [20] introduced a new geometry which is called 'helical swirl flow generator' and investigated the effect of the helical length of the swirl flow generator on the performance of the VT. Markal *et al.* [21] investigated the effects of the conical valve angle on energy separation in a VT.

Farouk *et al.* [22], used a computational fluid dynamic model to predict the species and temperature separation within a VT. A three dimensional Computational Fluid Dynamics (CFD) model is used by Dutta *et al.* [23] to investigate the phenomena of energy and species

separation in a VT with compressed air at normal atmospheric temperature and cryogenic temperatures as the working fluid.

The present study describes an experimental investigation on the effects of cold end orifice diameter, length and diameter of the tube in a counter-flow RHVT at various inlet pressures and Cold Fractions (CF) which was not reported before. This work aims to obtain the optimum values for these parameters which are responsible for larger temperature separation in a counter-flow RHVT. A symmetric numerical investigation of flow and temperature field within a counter-flow RHVT by the use of a Navier-Stokes model is presented to analyze the temperature separation effect in a counter-flow RHVT. Due to some operational limitation, all experiments were carried out at inlet pressure less than 347.9 kPa. For investigating the effect of higher inlet pressures (up to 1053 kPa) CFD models are extrapolated after validation.

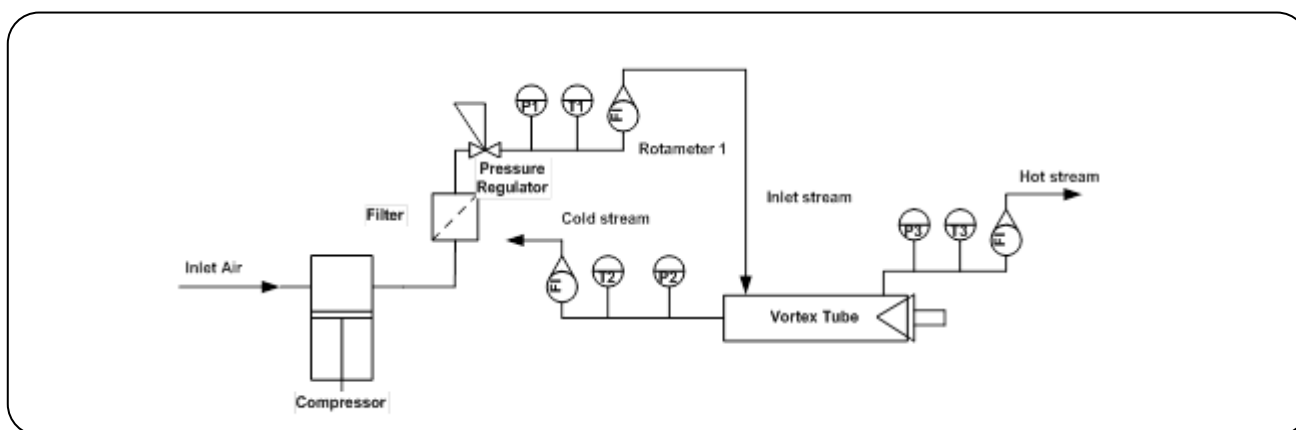
The present work novelty is the design and construction of a VT in such a way to be able to interchange all parts. This unique advantage provides the ability to investigate the effects of numerous parameters on VT performance simultaneously. Investigation of tube length and diameter effect on the VT performance as independent parameters (not as  $L/D$  ratio) by experiment and supported by CFD simulation is another novelty of the present work.

## EXPERIMENTAL SECTION

The experimental set up is shown in Fig. 2. A brass VT was constructed with dimensions as shown in Table 1.

**Table 1: Geometrical dimensions of vortex tube.**

Inner diameter	8-12 mm
Length	96-480 mm
Inlet Nozzlenumbers	4
Inlet Nozzle diameter	2 mm
Distances between nozzle intakes and cold end orifice	1 mm

**Fig. 2: The experimental setup.**

The experiments were performed in VTs with 4 inlet nozzle number and inlet nozzle diameter equal to 2 mm. Eight main tubes (made of brass) with following dimensions have been constructed:

Inner diameter (mm)/Length (mm): 8/240 -10/240-12/240-8/96-8/200-8/320-8/400-8/480

The cold end orifice diameter, length and diameter of VT are tested to obtain highest performance during the experiments.

The effect of the cold end orifice diameter is investigated by five different cold orifices with following diameters: 2, 3, 4, 5 and 8 mm; diameter and length of main tube are 8 and 240 mm, respectively.

To find optimized main tube dimensions (diameter and length), all main tubes with mentioned dimensions and 4 mm cold end orifice diameter have been used.

Experiments were carried out at room temperature (23°C). The compressed air after passing oil and water filter, pass through a regulator for adjusting inlet pressure (varied from 0.3 to 2 barg). The temperature, pressure and flow rate of the compressed air are measured after that. Then the compressed air enters tangentially into the VT where it is expanded and separated into hot and cold air streams. The cold stream in the central region flows

out of the tube through the cold end orifice close to the entrance while the hot stream exit from the outer periphery between the wall of the tube and the conical valve in the opposite end. Just after the pipe, the pressure, temperatures and flow rate are measured. The flow rate in both sides can be varied by the conical valve located at the hot end of the tube.

The air flow rate is measured with a Rotameter (BESTA DK800S-6, Korea) with an uncertainty of +/-1%. With these rotameters there is no need to compensate pressure and temperature, neglecting minor throttling effect. Temperature is measured by the RTD type thermometer (Pt 100 ITP, Italy) which are located at compressor outlet, VT inlet, cold and hot exit streams. For measuring pressure, there is a gauge with a 0-1.4 MPa range on the compressor. For pressure measurement, Piezo-sensor (BD 26.600G, Germany), with almost negligible pressure drop, are used at VT inlet, cold and hot exit streams, to measure their pressure.

Because of the slow response time of aforementioned thermometer, experimental data was not logged dynamically, so steady state data were used. Steady state is achieved when a less than 0.1°C temperature change is observed in two successive measurements.

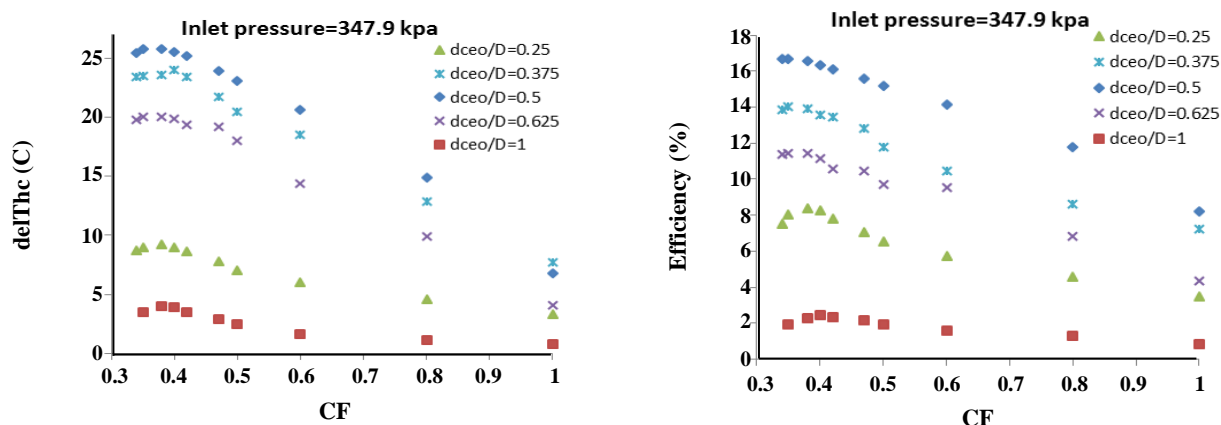


Fig. 3: Comparison of (a) hot - cold exit temperature difference (b) isentropic efficiency vs. CF for different cold end orifice diameter ( $d_{ceo}$ ) (Inlet pressure=347.9kPa, Number of nozzles=4,  $D_{nozzle}$ =2mm, distances between nozzle intakes and cold end orifice=1mm, VT diameter=8mm and VT length=240mm).

This increment is justified when compared to total errors and to the elapsed time to reach the steady temperatures.

The repeatability of the measurements was checked during multiple runs. The average deviation was calculated to be in the order of 0.53 °C.

## RESULTS AND DISCUSSION

### Experimental Results

#### Cold end orifice diameter

To investigate the effect of cold end orifice diameter, five different orifices were made ( $d_{ceo}$ : 2, 3, 4, 5 and 8mm). The difference between hot and cold exit temperature ( $\Delta T_{hc}$ ) versus different CF (cold flow to inlet flow ratio) at a specific constant inlet pressure (347.9kPa maximum available pressure) are illustrated in Fig.3(a). Note that CF=1 represents the state without hot outlet.

It is obvious that  $\Delta T_{hc}$  increases slightly with CF increase from 0.32 to 0.4 and there is an optimum value in range of  $0.4 < CF < 0.5$ , then decreases sharply for  $CF > 0.5$  regardless of cold end orifice diameter. The CF value of 0.4 (the simulations were done for cold end orifice diameter equal to 4mm) is chosen as the optimum value for CFD simulation.

It is also observed that  $\Delta T_{hc}$  in case of cold end orifice diameter equal to 4mm ( $d_{ceo}/D=0.5$ ) is the highest and in the case of cold end orifice diameter equal to 8mm ( $d_{ceo}/D=1$ ; no orifice) is the lowest.

Fig.3(b) shows the isentropic efficiency  $\{(T_i - T_c) / (T_i - T_s)\}$  with  $T_s = T_i (P_c / P_i)^{(C_p / C_v)}$  versus CF and diameter of cold end orifice.

The optimum cold end orifice diameter which provides highest isentropic efficiency would be 4mm (Fig 3b). The best performance of vortex tube occurred at a cold end orifice diameter of  $D/2$ . It is shown that as the cold end orifice diameter increases from 2 to 4mm ( $d_{ceo}/D=0.25$  to 0.5),  $\Delta T_{hc}$  is increased. On the other side, a diameter increase over 4mm ( $d_{ceo}/D=0.5$ ) would result a decrease in the performance of vortex tube. When the cold orifice diameter is smaller, higher pressure drop is generated and resulted in a poorer energy separation and when it is larger, the more hot gas is discharged into the cold gas and the cold gas temperature is increased so there should be an optimum value for cold end orifice diameter which is equal to 4mm.

The cooling power ( $Q_c$ ) as defined by Gao [22], only concerns the cold stream:

$$Q_c = m_c C_p (T_i - T_c) \quad (1)$$

The optimum cooling power per cold exit mass flow rate which is obtained at cold end orifice diameter of 4mm and  $CF=0.4$  by using the above equation is 12.9kJ/kg.

The Coefficient Of Performance (COP) is also reported as an evaluation criterion for VT:

$$COP_{cr} = Q_c / P \quad (2)$$

$$COP_{cn,cr} = T_c / (T_i - T_c) \quad (3)$$

Where  $Q_c$  is the system cooling power,  $COP_{cr}$  and  $COP_{cn,cr}$  [22] representing the Carnot COP and the maximum efficiency for the VT system respectively.  $P$  is the work used to compress the gas from the exhaust pressure up to the input pressure with a reversible isothermal compression process.

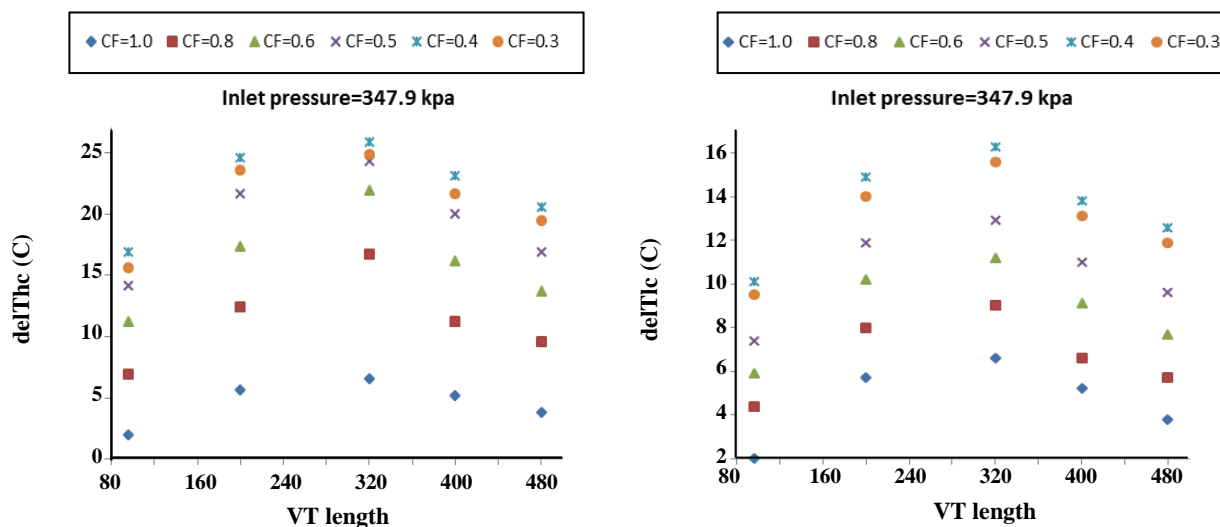


Fig. 4: Comparison of (a) hot - cold exit temperature difference (b) inlet - cold exit temperature difference vs. main tube lengths for different CF (Number of nozzles=4,  $D_{nozzle}=2mm$ , distances between nozzle intakes and cold end orifice=1mm, cold end orifice diameter=4mm and VT diameter=8mm).

$$P = m_i R_m T_i \ln(P_i/P_c) \quad (4)$$

At cold end orifice diameter = 4mm ( $d_{ceo}/D=0.5$ ) and CF=0.4, the optimum values of  $COP_{cr}$  and  $COP_{cn,cr}$  are obtained as 4.5 and 22.5 % respectively.

There has not been a unanimous interpretation for the significance of these definitions, as the cold stream contribution is a controversial subject.

#### Length of main tube effect

For investigating the effect of tube length, five tubes with different lengths but similar ID of 8mm are tested.

The difference between cold and hot exit temperature ( $\Delta T_{hc}$ ) and inlet and cold temperature ( $\Delta T_{ic}$ ) versus different main tube lengths (96, 200, 320, 400 and 480 mm) for different CFs at a specific constant pressure (347.9 kPa) are illustrated in Figs. 4(a) and (b) respectively.

As shown above, by increasing the main tube length from 96 to 320mm, the performance of the VT is improved. On the other hand as the main tube length raises from 320 to 480mm this performance is decreased. As a result, we can conclude that the best tube length is 320mm length regardless of CF values.

We can also see that  $\Delta T_{hc}$  and  $\Delta T_{ic}$  increases with CF increase from 0.3 to 0.4 and there is an optimum value for cold and hot exit temperature difference at CF=0.4. For CF>0.4, because the hot gas is mixed with the cold gas in the core region and leave the VT with cold

gas through the cold orifice, the amount of  $\Delta T_{hc}$  and  $\Delta T_{ic}$  decreases with increasing the CF.

#### Effect of vortex tube diameter

For studying the effect of tube diameter, three tubes with different diameter (8, 10 and 12mm) and similar length of 240mm are constructed.

Cold and hot exit temperature ( $T_c$ ,  $T_h$ ) versus different CFs at a specific constant pressure (347.9 kPa) are investigated and shown in Figs. 5 (a) and (b).

Fig.5 (a) shows that cold exit temperature increases slightly with the CF increase from 0.32 to 0.68 and reaches a maximum, then decreases for CF> 0.68 regardless of the tube diameter. The hot exit temperature (Fig.5 (b)) also increases with CF increase from 0.32 to 0.4 and reaches a maximum then decreases suddenly for CF> 0.4.

It is found that as the diameter decreases, the hot exit temperature in the vortex tube increases and the cold exit temperature decreases. When the VT diameter increases the outlet hot and cold streams will mix and the energy separation through the VT decreases, so the best performances among tested diameters are provided by a VT with inner diameter of 8mm.

#### Effect of length to diameter ratio

As mentioned above, eight tubes with different L/D were constructed (12, 20, 24, 30, 40, 50 and 60).

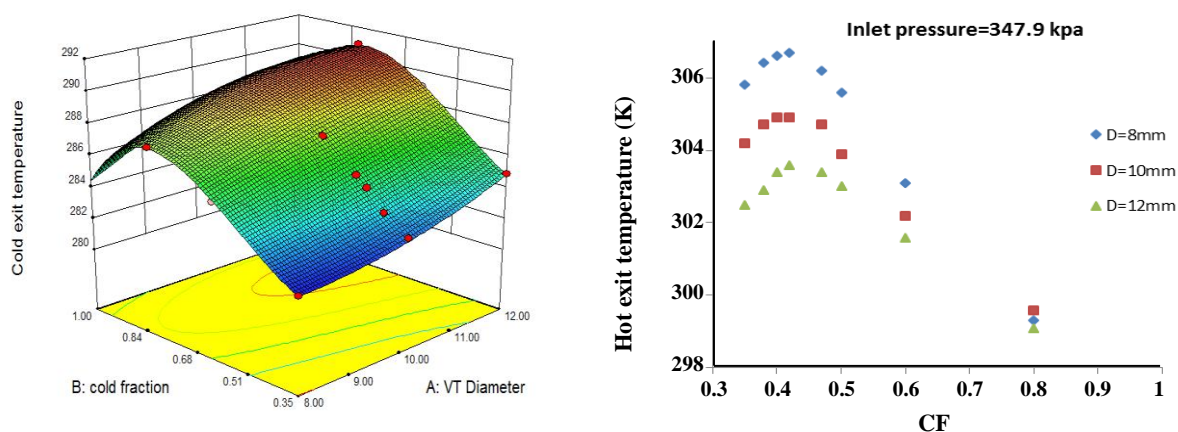


Fig. 5: (a) Cold exit temperature (b) Hot exit temperature difference vs. CF for different tube diameter (Number of nozzles=4,  $D_{nozzle}=2\text{mm}$ , distances between nozzle intakes and cold end orifice=1mm, cold end orifice diameter=4mm and VT length=240mm,  $T_{in}=296\text{K}$ ).

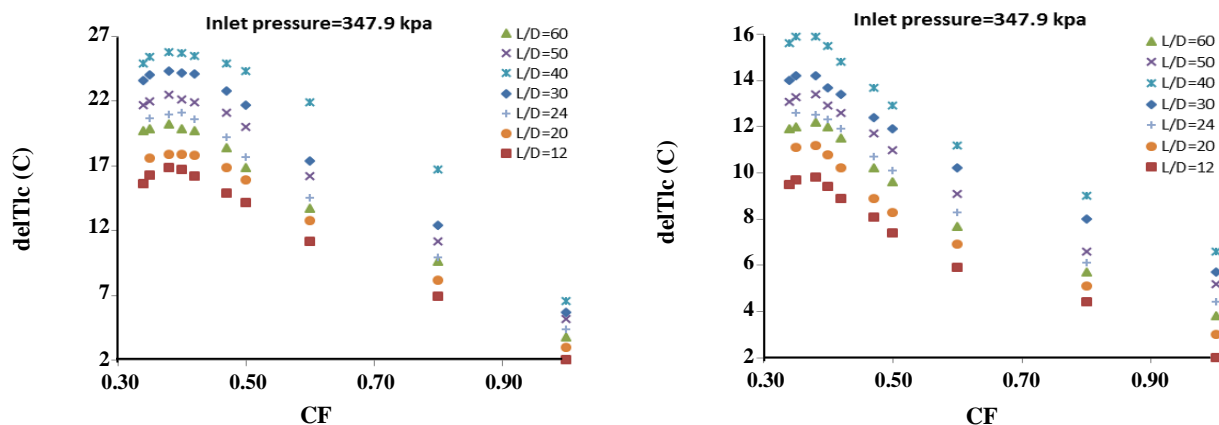


Fig. 6: Comparison of (a) hot - cold exit temperature difference (b) inlet - cold exit temperature difference vs. CF for tubes with different L/D (Number of nozzles=4,  $D_{nozzle}=2\text{mm}$ , distances between nozzle intakes and cold end orifice=1mm, cold end orifice diameter=4mm).

Difference between cold and hot exit temperature ( $\Delta T_{hc}$ ), inlet and cold temperature ( $\Delta T_{ic}$ ), versus different CFs at a specific constant pressure (347.9 kPa) are presented in Figs. 6 (a) and (b).

As shown, the performance of VT improves with the L/D increase from 12 to 40 and reaches an optimum, then decreases for the L/D more than 40 regardless of the CF, so the best performances occurred at L/D=40 (L=320mm and D=8mm).

L/D plays a critical role in mixing of the hot and cold streams. The hot gas moves peripheral and the cold gas moves through the core in the opposite direction. If the VT diameter is large and the VT length is small, the hot

and cold streams will mix. As *Behera et al.* [12] mentioned, when the VT length increases the energy separation is improved up to stagnation point along the tube. So, for the best VT performance, there should be an optimum value for L/D.

#### Effect of inlet pressure

The effect of inlet pressure ( $P_{in}$ ) in this section is investigated for a VT with Number of nozzles=4,  $D_{nozzle}=2\text{mm}$ , distances between nozzle intakes and cold end orifice=1mm, cold end orifice diameter=4mm, VT diameter=8mm and length=320mm, which correspond to the optimum values obtained so far. The dependency

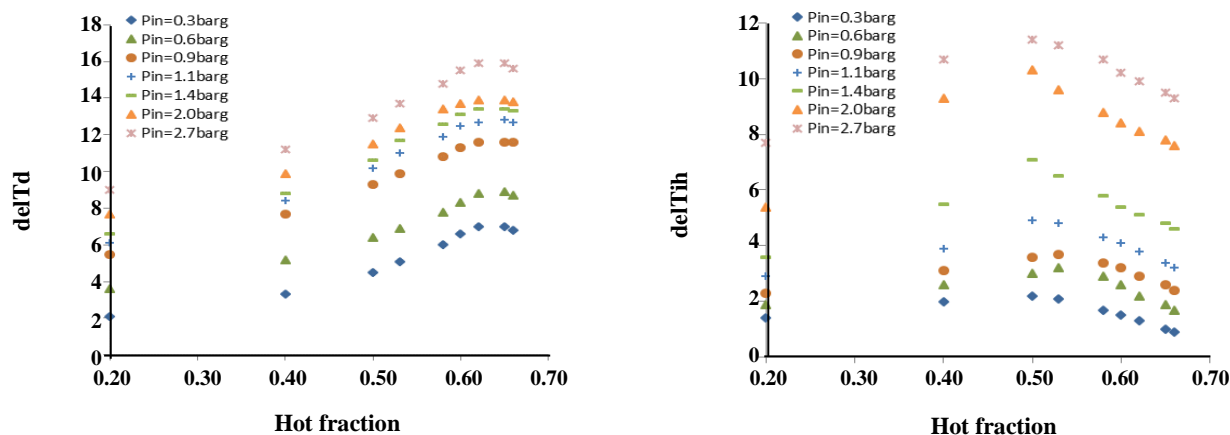


Fig. 7: Comparison of (a) inlet - cold exit temperature difference (b) inlet - hot exit temperature difference vs. hot fraction for different inlet pressure ( $D=8\text{mm}$ ,  $L=320\text{ mm}$ , cold end orifice diameter= $4\text{mm}$ , Number of nozzles= $4$ ,  $D_{\text{nozzle}}=2\text{mm}$  and distances between nozzle intakes and cold end orifice= $1\text{mm}$ ).

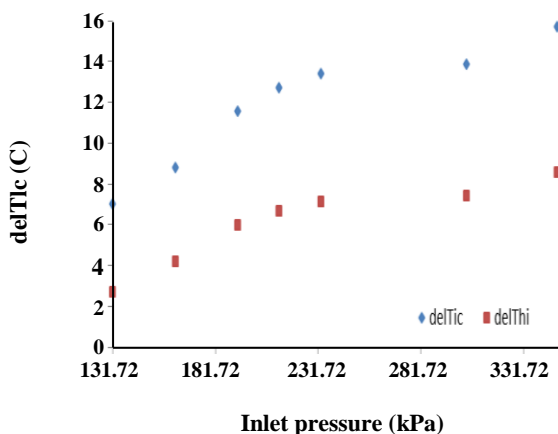


Fig. 8:  $\text{del}T_{\text{ic}}$  and  $\text{del}T_{\text{hi}}$  for different inlet pressure (hot fraction =  $0.62$ ,  $D=8\text{ mm}$ ,  $L=320\text{ mm}$ , cold end orifice diameter= $4\text{mm}$ , Number of nozzles= $4$ ,  $D_{\text{nozzle}}=2\text{mm}$  and distances between nozzle intakes and cold end orifice= $1\text{mm}$ ).

of  $\text{del}T_{\text{ic}}$ ,  $\text{del}T_{\text{hi}}$  versus hot fraction ( $1-\text{CF}$ ) for different inlet pressure is shown in Fig.7(a) and (b).

As shown above, that cold exit temperature decreases slightly with the hot fraction increase from  $0.2$  to  $0.62$  and reaches a minimum, then increases sharply regardless of inlet pressure. This trend is obviously reversed for the hot exit temperature (Figure 7 (b)). The hot exit temperature increases with CF increase from  $0.2$  to  $0.52$  and reaches a maximum then decreases suddenly.

For better evaluation of the pressure effect, a specific hot fraction is selected ( $0.62$ ), for which  $\text{del}T_{\text{ic}}$  and  $\text{del}T_{\text{hi}}$  versus the inlet pressure are illustrated in Fig. 8. It is seen

that at the given hot fraction by increasing the inlet pressure from  $131.7$  to  $347.9\text{ kPa}$ , the temperature of cold exit decreases and hot exit increases so the best performances occurred at the highest tested pressure of  $347.9\text{ kPa}$ , as reported in the literature by *Dincer et al.* [11] and *Gao* [22]. This is due to the fact that at high pressure, tangential velocity of VT entering gas is higher so the momentum transfer between core and periphery is increased. This causes an improved temperature separation, providing a higher temperature at the tube surface and a lower temperature in the core region of the tube.

#### CFD model

A 2-D model CFD has been developed with VT length of  $240\text{mm}$  and diameter of  $8\text{mm}$ , four nozzle intakes, nozzle diameter of  $2\text{mm}$  and cold end orifice diameter of  $4\text{mm}$  using the commercial CFD code *Fluent 6.3.26* (Fig.9). The air is chosen as an ideal working fluid with constant specific heat capacity, thermal conductivity, and viscosity. The inlet boundary conditions are fixed at temperature  $290\text{K}$  and pressure  $212.78\text{ kPa}$ . The pressure at the cold exit boundary is fixed to the atmospheric pressure and hot exit pressure is adjusted by varying the cold fraction.

Calculations are carried out assuming a 2-D axisymmetric compressible flow. Standard  $k-\epsilon$  and "ReNormalization Group" (RNG) version of  $k-\epsilon$  turbulence models (as the Reynolds number is very high) are used to solve the mass, momentum, and energy conservation equations to obtain the flow and thermal fields.

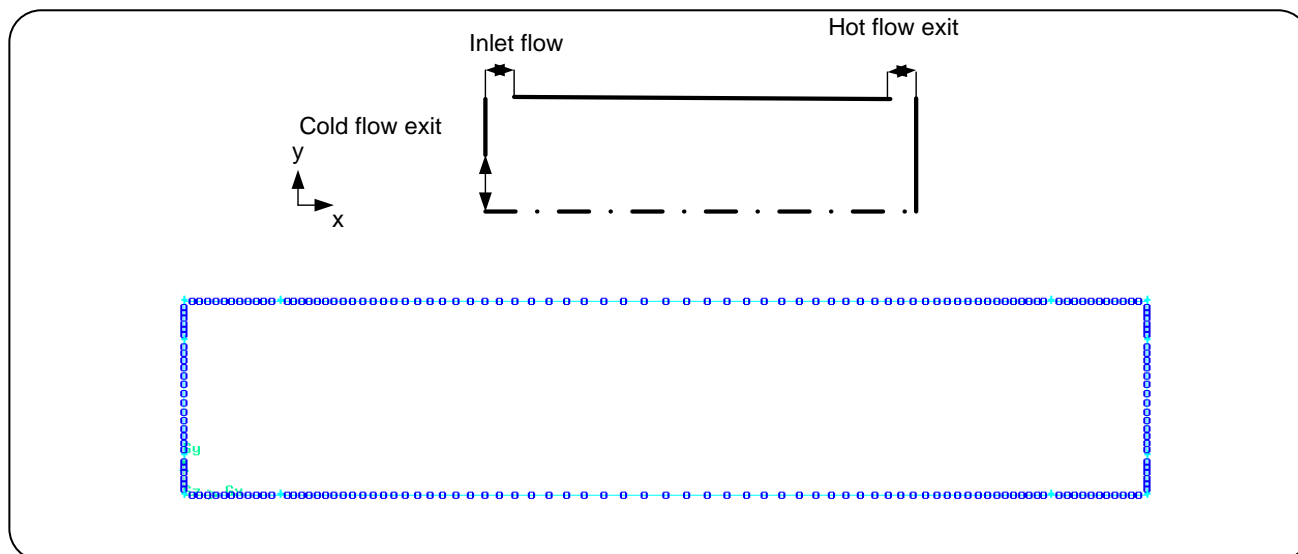


Fig. 9: Two dimensional CFD model, with grid distribution and streams configuration[25].

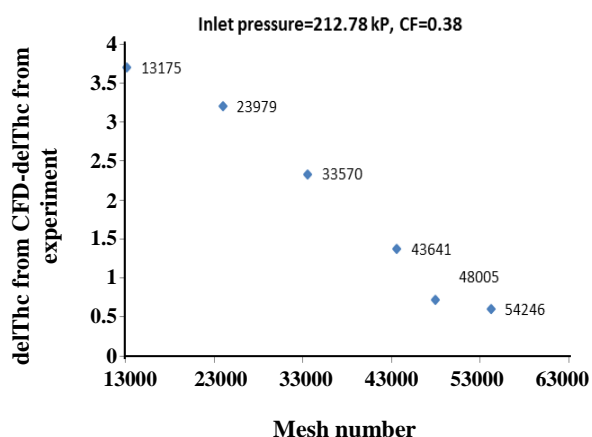


Fig. 10: Investigation of the mesh density dependency.

However it is found that using standard  $k-\varepsilon$  turbulence models for specified  $CF=0.38$ , the difference between the measured and predicted hot and cold exit temperature increases; advanced turbulence models such as the Reynolds stress equations could not converge ( $10^{-5}$  is considered as convergence criterion for velocity, energy, continuity,  $k$  and  $\varepsilon$ ). For this simulation RNG version of  $k-\varepsilon$  is used as turbulence model, as large centrifugal pressure gradients applies on the turbulence intensity. In these models, the gravity effects are omitted and in the solid boundaries no slip or adiabatic conditions exist. Boundary conditions which are used in these series of simulation are Stagnation boundary condition for the VT inlet with determined pressure and temperature

(obtained from the experiments) and pressure boundary for cold and hot exit.

These results are produced by using a mesh consisting of 54000 grid elements in longitudinal half of the tube. The results of investigation of the mesh independency indicated that the change of grid density does not affect the results, provided that 48000 or more mesh elements are considered (Fig. 10). The grid concentration of the mesh is adaptively selected such that it is high in the regions where large gradients in the velocity or pressure may exist (Fig. 9), specifically in the inlet plane as well as in the hot and cold zones.

#### Validation

Here the comparison is made between the temperature separations achieved from the present numerical evaluations by use of air as working fluid with experimental data. Good results were obtained from applying  $k-\varepsilon$  turbulence models in analyzing a vortex tube complex flow field.

The fixed parameters throughout the numerical study are listed in Table 2. Simulations are performed with varying the hot exit pressure boundary values at eight different cold fractions so the hot gas outlet pressure parameter was changed during the CFD evaluations.

Figs. 11 (a) and (b), show the difference between cold and hot exit temperature ( $\Delta T_{hc}$ ) and the difference between hot exit and inlet temperature ( $\Delta T_{hi}$ ), versus  $CF$  at a specific inlet pressure (212.78 kPa) respectively.



**Table 2: Fixed parameters for the vortex tube simulation.**

parameter	value
Cold exit pressure (kPa)	101.325
Inlet pressure (kPa)	165.5
Inlet radial velocity (m/s)	20
Inlet total temperature (K)	290
Inlet azimuthal velocity (m/s)	200

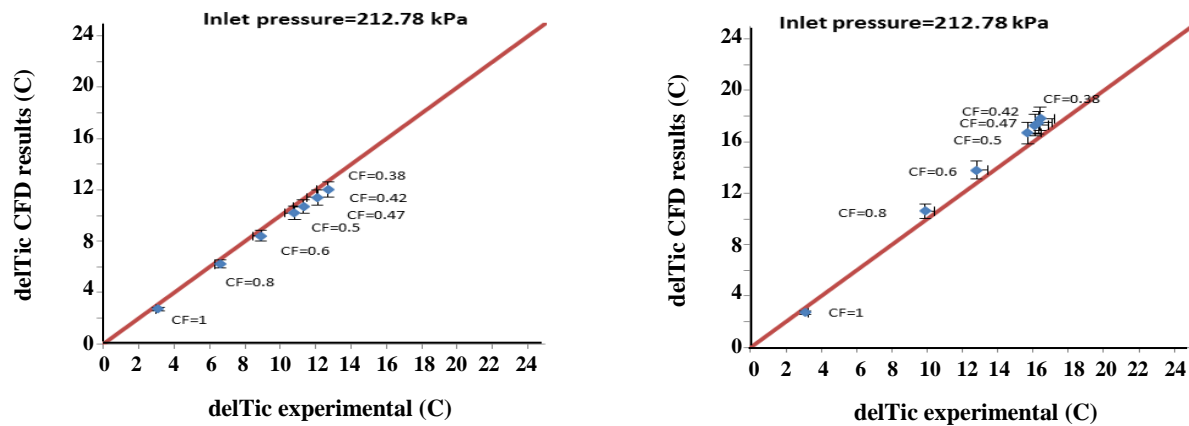


**Fig. 11: Comparison of (a) inlet - cold exit temperature difference ( $R^2=0.9998$ ) (b) cold - hot exit temperature difference ( $R^2=0.9993$ ) of CFD simulation with the experimental data (number of nozzles = 2,  $D_{nozzle}=2\text{mm}$  and distances between nozzle intakes and cold end orifice = 1mm).**

In these figures data achieved by present CFD model is validated against the experimental results.

It is observed that the predictions obtained from this study are close to the experimental results. (5.51 and 7.2% deviations respectively)

CFD model shows that a maximum hot exit temperature of 300 K at CF=0.42 is produced.

It seems that the reason of observed difference between experimental and CFD results is the experiment's deviation from ideal assumptions, the implementation of which is quite difficult, to name but a few the residual frictional losses and adiabatic conditions.

#### Temperature and tangential velocity field

The contour plot of the predicted temperature is shown in Fig. 12 (a). where hot and cold regions can be clearly observed. As seen in Fig. 12 (a), a maximum is observed close to the tube wall beyond which temperature decreases. This maximum point also represents the stagnation point as defined by Fulton [26]. He stated that

at this point, the tube wall is hotter than the outlet mixed air, and hotter than the tube wall either at the inlet or at the far end of the tube. Here, it is shown with an increase at the inlet pressure, this point is displaced closer in the axial direction.

At the CF of 0.42 a minimum cold temperature of 281K was obtained with relevant contours illustrated in Fig. 12 (a).

The contour plot of the predicted tangential velocity is also shown in Fig. 12 (b). The fluid (air) with high tangential velocity is entered to the VT, where according to some theories the friction between gas layers causes the temperature separation and the conversion of tangential velocity to axial velocity along the VT length. As seen in less than a fourth of VT length for this specific CF, the tangential velocity is totally disappearing and longitudinal velocity becomes predominant.

#### Effect of vortex tube diameter

To compare the CFD results of VT with experimental data, three 2-D models with different VT diameters (8, 10 and 12mm)

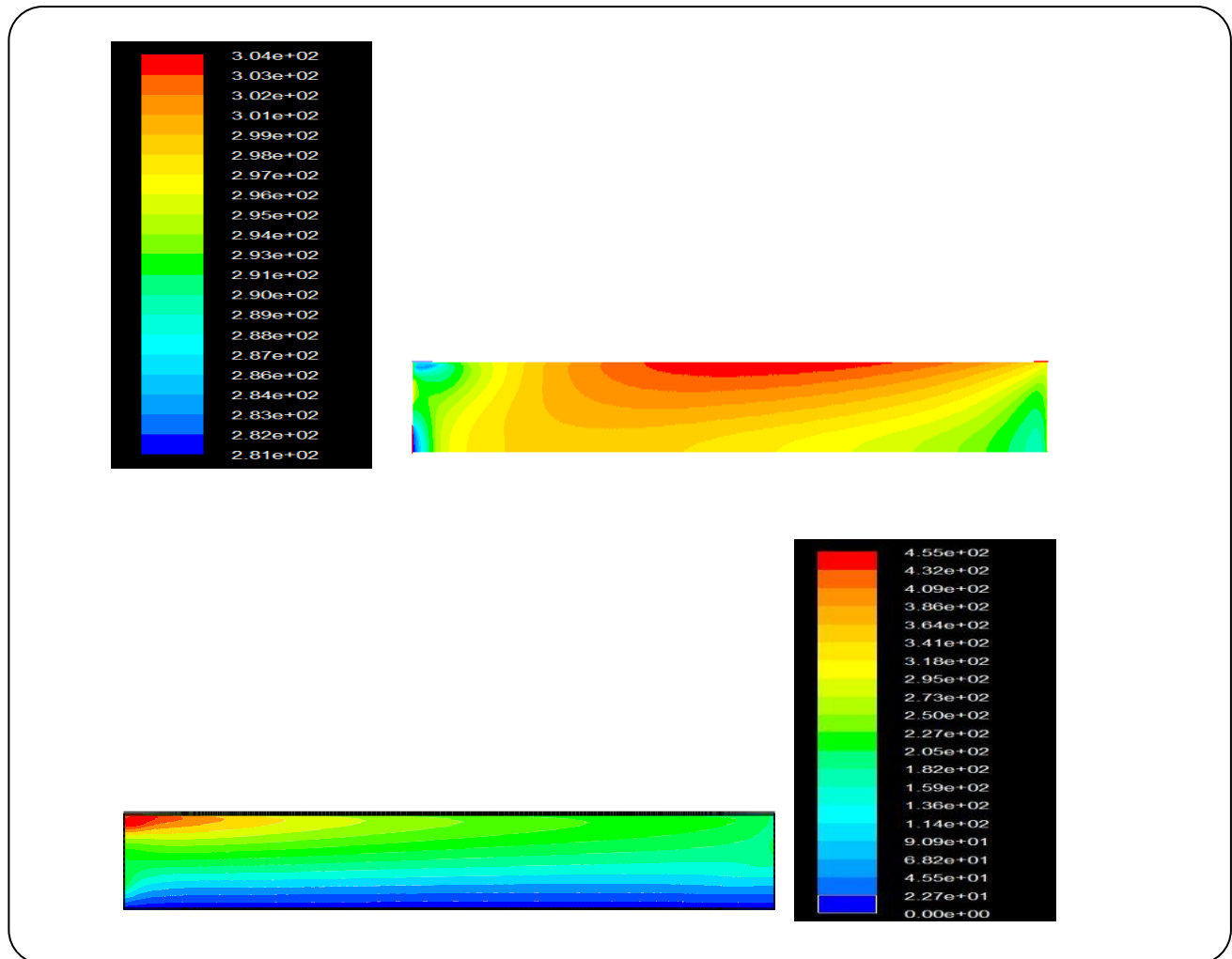


Fig. 12: Contour plot of predicted (a) temperature (K) [25] (b) tangential velocity (m/s) for vortex tube at  $CF=0.42$ .

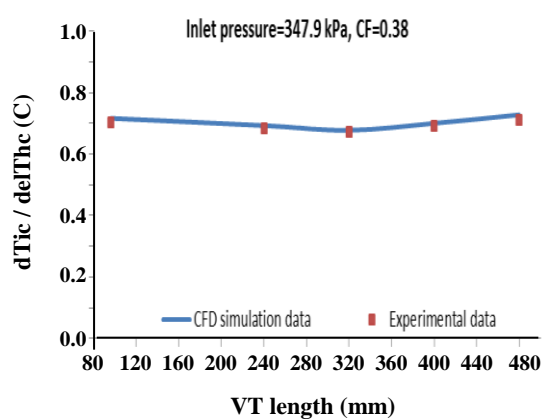


Fig. 13: Comparison of  $dT_{hc}/T_i$  in CFD simulation and experimental results ( $R^2=0.9943$ ) (cold end orifice diameter=4mm, Number of nozzles=4,  $D_{nozzle}=2mm$  and distances between nozzle intakes and cold end orifice=1mm).

has been developed. The obtained results are shown in Fig. 13. For these tests, inlet pressure is equal to 347.9 kPa (maximum available pressure) and  $CF=0.4$  (as the minimum cold exit temperature is produced at about this  $CF$ ), cold end orifice diameter is 4mm, Number of nozzles=4,  $D_{nozzle}=2mm$  and distances between nozzle intakes and cold end orifice=1mm.

In Fig. 13 CFD generated data for VTs with different diameters are compared with the experimental results. It is found that as the diameter decreases, the difference between hot and cold exit temperature in the vortex tube increases. With diameter increase, the outlet hot and cold streams will mix and the energy separation through the VT decreases, so the best performances among tested diameters are provided with VT inner diameter of 8mm.

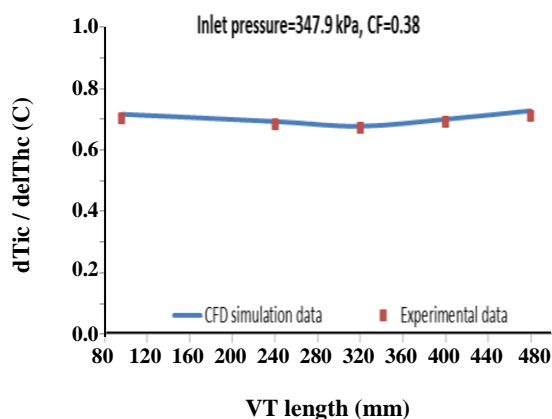


Fig. 14: Comparison of cold and hot exit temperature difference ( $\Delta T_{ic} / \Delta T_{hc}$ ) vs. VT length in experimental results ( $R^2=0.9934$ ) (cold end orifice diameter=4mm, Number of nozzles=4,  $D_{nozzle}=2$ mm and distances between nozzle intakes and cold end orifice=1mm).

#### Effect of vortex tube length

To compare the results of VT length effect in experimental test and CFD simulation, five 2-D models with different VT lengths (96, 240, 320, 400 and 480mm) have been developed. The obtained results are shown in Fig. 14. In these tests, inlet pressure is equal to 347.9 kPa (maximum available pressure) and  $CF=0.4$  (because minimum cold exit temperature is produced at about this  $CF$ ), cold end orifice diameter=4mm, Number of nozzles=4,  $D_{nozzle}=2$ mm and distances between nozzle intakes and cold end orifice=1mm respectively.

Fig. 14, presents the  $\Delta T_{ic} / \Delta T_{hc}$  versus VT length at a specific inlet pressure and  $CF=0.4$  (because minimum cold exit temperature is produced at about this  $CF$ ). It is seen there is an optimum value for tube length equal to 320mm. When the VT length increases the energy separation is improved up to a stagnation point along the tube. Although there are some quantitative divergences, the model captures the physical trends of the system behavior.

#### Effect of inlet pressure

To investigate the effect of increasing the inlet pressure on the thermal separation in RHVT, Two dimensional models with different inlet pressure has been developed. (Fig. 15). In these models,  $CF=0.4$  (as the minimum cold exit temperature is produced at about this  $CF$ ), cold end orifice diameter=4mm, Number of

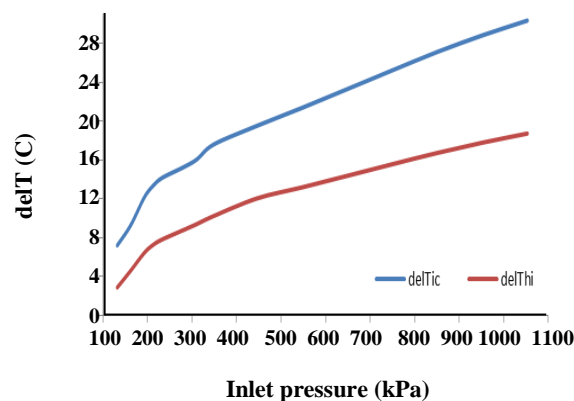


Fig. 15: Comparison of  $\Delta T_{ic}$  and  $\Delta T_{hi}$  vs. different inlet pressure in CFD results (cold end orifice diameter=4mm, Number of nozzles=4,  $D_{nozzle}=2$ mm and distances between nozzle intakes, cold end orifice=1mm and  $CF=0.4$ ).

nozzles=4,  $D_{nozzle}=2$ mm and distances between nozzle intakes VT length= and cold end orifice=1mm respectively. Due to some operational limitation, all experiments have been carried out at inlet pressure less than 347.9 kPa. For inlet pressure up to 1053kPa CFD simulation provides the performance shown in Fig. 15. CFD simulation is used not only for investigating the effect of higher inlet pressure, but also to investigate unknown field such as mass transfer in condensate separation.

Fig. 15, presents the  $\Delta T_{ic}$  and  $\Delta T_{hi}$  versus inlet pressure at the specific  $CF=0.4$ . The results show that by inlet pressure increase, the VT performance is improved (cold exit temperature decrease and hot exit temperature increase).

## CONCLUSIONS

By the experimental analysis, energy separation in a vortex tube has been studied and the optimum values of cold end orifice diameter, main tube diameter and length are obtained. It is concluded that, there is an optimum value for cold end orifice diameter. Among various cold end orifice diameter (2, 3, 4, 5, 8 mm), vortex tube with cold end orifice diameter of 4mm ( $D/2$ ) has the best performance.

There is an optimum value for VT diameter as well. Among various VT diameters (8, 10 and 12 mm), VT with diameter of 8 mm has the highest performance.

The effect of VT main length is also investigated in this work (96, 200, 320, 400 and 480 mm). It is found that VT with main tube length equal to 320mm is having the best performance.

Effect of inlet pressure variation on VT performance is also investigated. It was observed that increasing the inlet pressure causes an increase of the hot exit temperature, while a decrease of the cold exit temperature.

Within the framework of CFD analysis, energy separation in a vortex tube has been studied. In this approach, there is a kind of axisymmetric geometry and continuous state flow, and for that aim, the standard k- $\epsilon$  turbulence model is used for indication of turbulent flow structure of the flow inside the vortex tube. The effect of VT diameter and length are also investigated by CFD and good agreement between experimental and CFD simulation result is observed. With the fine-tuned CFD model, one can extrapolate the VT process parameters to unknown fields.

The effect of VT diameter is also investigated by CFD and good agreement between CFD simulation and experimental results is observed and optimum nozzle diameter equal to 8mm is confirmed.

By using experimental and CFD simulation results, the optimum value of VT length is also found (320mm).

### Nomenclature

CF	Cold fraction, $m_c/m_i$
$C_p$	Specific heat capacity, J/(kg K)
COP	Coefficient of performance
$COP_{cr}$	Cooler coefficient of performance
D	Tube inside diameter, m
$d_{ceo}$	Cold end orifice diameter, m
L	Main tube length, m
m	Mass flow rate, kg/s
P	Work power, J/kg
$Q_c$	Cooling power, J/kg
$R_m$	Specific gas constant, J/(mol K)

### Subscripts

c	Cold exit
i	Inlet
h	Hot exit
s	Isentropic

### REFERENCES

- [1] Kurosaka M., Acoustic Streaming in Swirl Flow and the Ranque-Hilsch (Vortex Tube) Effect, *J. Fluid Mech.*, **124**: 139-172 (1982).
- [2] Ahlborn B.K., Groves S., Secondary Flow in a Vortex Tube, *Fluid Dyn. Res.*, **21**: 73-86 (1997).
- [3] Hilsch R., The Use of the Expansion of Gases in A Centrifugal Field as Cooling Process, *Rev. Sci. Instrum.*, **18**(2): 108-113 (1947).
- [4] Ahlborn B.K., Gorden J.M., The Vortex Tube as A Classic Thermodynamic Refrigeration Cycle, *J. Appl. Phys.*, **88** (6): 3645-3653 (2000).
- [5] Gao C.M., Bosschart K.J., Zeegers J.C., de Waele A.T.A.M., Experimental Study on a Simple Ranque- Hilsch Vortex Tube, *Cryogenics*, **45**: 173-183 (2005).
- [6] Deissler R.G., Perlmutter M., Analysis of the Flow and Energy Separation in a Turbulent Vortex, *Int. J. Heat Mass Transfer*, **1**: 173-191 (1960).
- [7] Frohlingsdorf W., Unger H., Numerical Investigations of the Compressible Flow and Energy Separation in the Ranque-Hilsch Vortex Tube, *Int. J. Heat Mass Transfer*, **42**: 415-422 (1999).
- [8] Amitani, T. Adachi, T. Kato. A Study on Temperature Separation in a Large Vortex Tube, *Transaction of JSME.*, **49**: 877-884 (1983).
- [9] Aljuwayhel N.F., Nellis G.F., Klein S.A Parametric and Internal Study of the Vortex Tube Using A CFD Model, *Int. J. Refrigeration*, **28** (3): 442-450 (2005).
- [10] Eiamsa-ard S., Wongcharee K., Promvong P., Experimental Investigation on Energy Separation in a Counter-Flow Ranque-Hilsch Vortex Tube: Effect of Cooling a Hot Tube, *Int. Communications in Heat and Mass Transfer*, **37**: 156-162 (2010).
- [11] Dincer K., Tasdemir, S. Baskaya S., Uysal B.Z., Modeling of the Effect of Length to Diameter Ratio and Nozzle Number on the Performance of Counter Flow Ranque-Hilsch Vortex Tube Using Artificial Neural Networks, *Applied Thermal Engineering*, **28**: 2380-2390 (2008).
- [12] Behera U., Paul P.J., Kasthuriangan S., Karunanithi R., Ram S.N., Dinesh K., Jacob S., CFD Analysis and Experimental Investigations Towards Optimizing the Parameters of Ranque-Hilsch Vortex Tube, *J. Heat and Mass Transfer*, **48**, 1961-1973 (2005).

Received : Jun. 16, 2015 ; Accepted :

- [13] Xue Y., Arjomandi M.R., Kelso R., A Critical Review of Temperature Separation in a Vortex Tube, *Experimental Thermal and Fluid Science*, **34**: 1367-1374 (2010).
- [14] Dutta, T. Sinhamahapatra K.P., Bandyopdhyay S.S., Comparison of Different Turbulence Models in Predicting the Temperature Separation in a Ranque–Hilsch Vortex Tube, *Int. J. Refrigeration*, **33**: 783-793 (2010).
- [15] Secchiaroli A., Ricci R., Montelpare S., D’Alessandro V., Numerical Simulation of Turbulent Flow in a Ranque–Hilsch Vortex Tube, *International Journal of Heat and Mass Transfer*, **52**: 5496–5511 (2009).
- [16] Aydın O., Baki M., An Experimental Study on the Design Parameters of a Counterflow Vortex Tube, *Energy*, **31**: 2763–277 (2006).
- [17] Nimbalkar S.U., Muller M.R., An Experimental Investigation of the Optimum Geometry for the Cold End Orifice of A Vortex Tube, *Applied Thermal Engineering*, **29**: 509-514 (2009).
- [18] Dincer K., Baskaya S., Uysal B.Z., Ucgul I., Experimental investigation of the Performance of A Ranque–Hilsch Vortex Tube with Regard to A Plug Located at the Hot Outlet, *Int. J. Refrigeration*, **32**: 87-94 (2009).
- [19] Kirmaci V., Exergy Analysis and Performance of A Counter Flow Ranque–Hilsch Vortex Tube Having Various Nozzle Numbers at Different Inlet Pressures of Oxygen and Air, *Int. J. Refrigeration*, **32**: 1626-1633 (2009).
- [20] Aydın O., Markal B., Avc M., A New Vortex Generator Geometry for A Counter-Flow Ranque-Hilsch Vortex Tube, *Applied Thermal Engineering*, **30**: 2505-2511 (2010).
- [21] Markal B., Aydın O., Avc M., An Experimental Study on the Effect of the Valve Angle of Counter-Flow Ranque–Hilsch Vortex Tubes on Thermal Energy Separation, *Experimental Thermal and Fluid Science*, **34**: 966–971 (2010).
- [22] Gao C., Experimental Study on the Ranque-Hilsch Vortex Tube, *Technische Universiteit Eindhoven*, (2005).
- [23] Farouk T., Farouk B., Gutsol A., Simulation of Gas Species and Temperature Separation in the Counter-Flow Ranque-Hilsch Vortex Tube Using the Large Eddy Simulation Technique, *International Journal of Heat and Mass Transfer*, **52**: 3320-3333 (2009) .
- [24] Dutta T., Sinhamahapatra K.P., Bandyopadhyay S.S., Numerical Investigation of Gas Species and Energy Separation in the Ranque–Hilschvortex Tube Using Real Gas Model, *International Journal of Refrigeration*, **34**(8): 2118-2128 (2011).
- [25] Mohammadi S., Farhadi F., Experimental Analysis of A Ranque-Hilsch Vortex Tube for Optimizing Nozzle Numbers and Diameter, *Applied Thermal Engineering*, **61**(2): 500-506 (2013).
- [26] Fulton C.D., Ranque’s Tube, *J American Society of Refrigerating Engineers*, **58**: 473-479 (1950).